ACTA PHYSIOLOGICA

Acta Physiol 2012, **204,** 403–418

Membrane cycling after the excess retrieval mode of rapid endocytosis in mouse chromaffin cells

A. E. Perez Bay,* A. V. Belingheri, Y. D. Álvarez and F. D. Marengo

Laboratorio de Fisiología y Biología Molecular, Departamento de Fisiología y Biología Molecular y Celular, Instituto de Fisiología, Biología Molecular y Neurociencias (CONICET), Facultad de Ciencias Exactas y Naturales, Universidad de Buenos Aires, Buenos Aires, Argentina

Received 18 April 2011,
revision requested 27 May 2011,
revision received 10 June 2011,
accepted 13 July 2011
Correspondence: F. D. Marengo, Laboratorio de Fisiología y Biología Molecular, Departamento de Fisiología y Biología Molecular y Celular, Instituto de Fisiología, Biología Molecular y Neurociencias, Facultad de Ciencias Exactas y Naturales – Universidad de Buenos Aires, Ciudad Universitaria, Pabellón II, 2° piso, Buenos Aires CP: 1428, Argentina.
E-mail: fernando@fbmc.fcen.uba.ar

*Present address: Department of Ophthalmology, Dyson Vision Research Institute, Weill Medical College, Cornell University, New York, New York, USA.

Abstract

Aim: After exocytosis, neuroendocrine cells and neurones keep constant the plasma membrane and the releasable vesicle pools by performing endocytosis and vesicular cycling. Patch-clamp capacitance measurements on chromaffin cells showed that strong Ca^{+2} entry activates excess retrieval: a rapid endocytosis process that retrieves more membrane than the one fused by preceding exocytosis. The main purpose of the present experiments was to study the recycling pathway that follows excess retrieval, which is unknown.

Methods: Membrane recycling after exocytosis–endocytosis can be studied by fluorescence imaging assays with FM1-43 (Perez Bay *et al. Am J Physiol Cell Physiol* 2007; 293, C1509). In this work, we used this assay in combination with fluorescent dextrans and specific organelle-targeted antibodies to study the membrane recycling after excess retrieval in mouse chromaffin cells.

Results: Excess retrieval was observed after the application of high-K^+ or cholinergic agonists during 15 or 30 s in the presence of FM1-43. We found that the excess retrieval membrane pool (defined as endocytosis–exocytosis) was associated with the generation of a non-releasable fraction of membrane (up to 30% of plasma membrane surface) colocalizing with the lysosomal compartment. The excess retrieval membrane pool followed a saturable cytosolic Ca^{2+} dependency, and it was suppressed by inhibitors of L-type Ca^{2+} channels, endoplasmic reticulum Ca^{2+} release and PKC.

Conclusion: Excess retrieval is not associated with the cycling of releasable vesicles, but it is related to the formation of non-releasable endosomes. This process is activated by a concerted contribution of Ca^{2+} entry through L-channels and Ca^{2+} release from endoplasmic reticulum.

Keywords calcium signal, endocytosis, exocytosis, FM1-43, membrane cycling.

Physiological relevance

In this work, we provide the first direct data about the fate of internalized membrane after excess retrieval. We show that excess retrieval is associated with the formation of non-releasable endosomes colocalizing with the lysosomal compartment. An expected consequence of this scenario is that under conditions of intense exocytosis followed by excess retrieval, a fraction of the releasable pool of vesicles will not recycle directly and will have to be recovered '*de novo*'.

In addition, our data contribute to understand other aspects associated with regulation of excess retrieval: we confirm the strong Ca^{2+} dependency of excess retrieval, but adding significant information about the shape of this dependence, and on the critical participation of Ca^{2+} release from endoplasmic reticulum, and PKC.

In neuroendocrine cells and neurones, calcium-dependent exocytosis generates an increase in plasma membrane surface and a depletion of releasable vesicle pools. In consequence, endocytosis and vesicular cycling are critical for maintaining membrane homoeostasis and secretion reliability (Burgoyne 1995, Koval *et al.* 2001, Artalejo *et al.* 2002). Capacitance measurements of membrane retrieval in bovine chromaffin cells revealed that a variety of stimuli can activate a rapid endocytosis process (Artalejo *et al.* 1995, Smith & Neher 1997, Nucifora & Fox 1998). Rapid endocytosis is a calcium-dependent process that is completed in approx. 20 s, and often retrieves a larger amount of membrane than the one added by preceding exocytosis (i.e. excess retrieval) (Artalejo *et al.* 1995, 2002, Smith & Neher 1997). It was proposed that rapid endocytosis may be coupled to a short vesicle cycle, particularly kiss and run, leading to a quick refilling of vesicle pools after exocytosis (Artalejo *et al.* 2002, Elhamdani *et al.* 2006). However, kiss and run is supposed to involve equal amounts of fused and retrieved membrane, whereas rapid endocytosis frequently displays excess retrieval. This suggests that other process or processes should contribute to rapid endocytosis. Moreover, it has been proposed that rapid endocytosis can be divided into two modes: compensatory endocytosis and excess retrieval, supposedly produced by two different mechanisms with different purposes (Smith & Neher 1997, Engisch & Nowycky 1998). While rapid compensatory endocytosis seems to be a mechanism involved in vesicular recycling during normal secretory activity (Smith & Neher 1997, Engisch & Nowycky 1998), the function of excess retrieval is still unclear.

Whole-cell capacitance measurements have been extensively used to study rapid endocytosis and excess retrieval because of its high temporal resolution (Artalejo *et al.* 1995, von Gersdorff & Matthews 1997, Smith & Neher 1997, Engisch & Nowycky 1998). However, this technique does not provide information regarding the post-endocytic membrane cycling. In this work, we approached this problem using the styryl dye FM1-43 to study excess retrieval and the fate of the membrane internalized during this process. In particular, it is important to know whether the internalized membrane is rapidly cycled or not to releasable vesicles. This is a relevant issue, because it will affect the secretory performance of chromaffin cells. To this end, we took advantage of a protocol introduced by us previously (Perez Bay *et al.* 2007), which allows to estimate in a single cell the exocytosis, the endocytosis and the fraction of internalized membrane recycled to releasable vesicles. We have previously demonstrated that prolonged stimulation (3 min) of chromaffin cells causing massive exocytosis (approx. 50% of the plasma membrane surface) is followed by compensatory endocytosis resulting in rapid releasable and non-releasable membrane pools, the latter likely generated by bulk endocytosis (Perez Bay *et al.* 2007). Here, we used shorter (≤30 s) stimuli (high-K^+ or cholinergic agonists) that allowed us to consistently observe a transient excess retrieval, similar in size to that observed by capacitance measurements under similar conditions. We defined the excess retrieval membrane pool (ERMP) as the fraction of internalized membrane exceeding previous exocytosis (i.e. endocytosis–exocytosis). We found that although an important amount of the total internalized membrane rapidly recycled to releasable vesicles, ERMP was tightly associated with the generation of non-releasable endosomes. ERMP was highly dependant on cytosolic calcium but independent of previous exocytosis size. The internalization of ERMP was triggered by Ca^{2+} entry through L-type channels combined with Ca^{2+} release from endoplasmic reticulum.

Materials and methods

All animal procedures are in accordance with the National Institute of Health Guide for the Care and Use of Laboratory Animals (NIH publication 80-23/96), USA, and local regulations. All efforts were made to minimize animal suffering and to reduce the number of animals used.

Cell culture and solutions

We extracted adrenal glands from two 12- to 18-day-old mice anesthetized with an avertine overdose following the procedures described in the study of Perez Bay *et al.* (2007). The medulla was removed mechanically from the cortex, digested for 25 min in 200 μL Hanks' solution containing papain (0.5–1 mg mL^{-1}) at 37 °C and subsequently disrupted in papain-free Dulbecco's modified Eagle's medium low glucose (D-MEM). The cell suspension was brought to a final volume of 600 μL D-MEM, filtered through 200- and 50-μm pore meshes and cultured on small pieces of poly-L-lysine-pre-treated coverslips at 37 °C, 95% O_2–5% CO_2 in D-MEM and were used for experiments 24–48 h later. D-MEM was supplemented with 5% foetal calf serum, 1 mg mL^{-1} bovine serum albumin, 10 μM cytosine-1-β-arabinofuranoside, 5 μL mL^{-1} penicillin/streptomycin and 1.3 μL mL^{-1} gentamicin. The standard solution used for the imaging experiments contained 145 mM NaCl, 5.6 mM KCl, 1.2 mM $MgCl_2$, 10 mM HEPES, 2 mM $CaCl_2$ and 10 mM dextrose. To stimulate cells, we used alternatively the following modifications of the standard solution: (i) for high K^+ depolarizations, 50 mM KCl in replacement of NaCl; (ii) for stimulation with cholinergic agonists, addition of 200 μM nicotine or carbachol. If not mentioned

explicitly (Fig. 5), stimuli were always applied in the presence of 2 mM external Ca^{2+}. For patch clamp experiments, the external solution was composed of (in mM) 120 NaCl, 20 Hepes, 4 $MgCl_2$, 5 $CaCl_2$, 5 mg mL^{-1} glucose and 1 μM tetrodotoxin (pH 7.3), and the standard internal solution contained (in mM) 95 Cs D-glutamate, 23 Hepes, 30 CsCl, 8 NaCl, 1 $MgCl_2$, 2 Mg-ATP, 0.3 GTP and 0.3 Cs-EGTA 6 (pH 7.2). All the experiments were at room temperature (22–24 °C).

Imaging techniques to measure exocytosis, endocytosis and vesicle recycling

Live imaging studies of exocytosis, endocytosis and vesicle recycling with FM1-43 were carried out with a BX50 WI Olympus microscope equipped with a 40× water-immersion objective (NA 0.8), epifluorescence illumination through a mercury lamp, a filter block (460- to 490-nm excitation filter, 505-nm dichroic mirror, 515-nm high pass filter) and a Quantix CCD camera (Photometrix, Tucson, AZ, USA; Perez Bay *et al.* 2007). Before the beginning of each experiment, we quantified the non-specific FM1-43 staining (Perez Bay *et al.* 2007), which was later subtracted from all experimental values.

Figure 1 represents a typical experiment performed on a single chromaffin cell. Figure 1(a) shows the epifluorescence images (always at the equatorial cell section) obtained at the end of the different stages of the protocol, and Figure 1(b) represents the time course of the spatially averaged cell fluorescence after subtraction of the non-specific staining. First, cells were incubated for 15 min in standard solution with FM 1-43 (5 μM), and a clear fluorescence plateau was established at the end of this period (I). Next, cells were stimulated (in this example, for 60 s with 50 mM K^+), still in the presence of FM1-43, to cause massive vesicular fusion to the plasma membrane. Because the quantum yield of FM1-43 dramatically increases when this fluorophore is inserted in the membrane, the augment in fluorescence (II) reveals the relative increase in membrane surface provoked by exocytosis (Exo1; Smith & Betz 1996). Subsequently, extracellular FM 1-43 was washed out with standard solution during 30 min to attain a new plateau (III), which is the result of the FM1-43 trapped in the fraction of membrane internalized by endocytosis (Endo) during the previous stimulation period. Finally (IV), a second stimulus (50 mM K^+ during 30 min) provoked a decay in cellular fluorescence (Exo2) owing to exocytosis and release of FM 1-43 attached to the

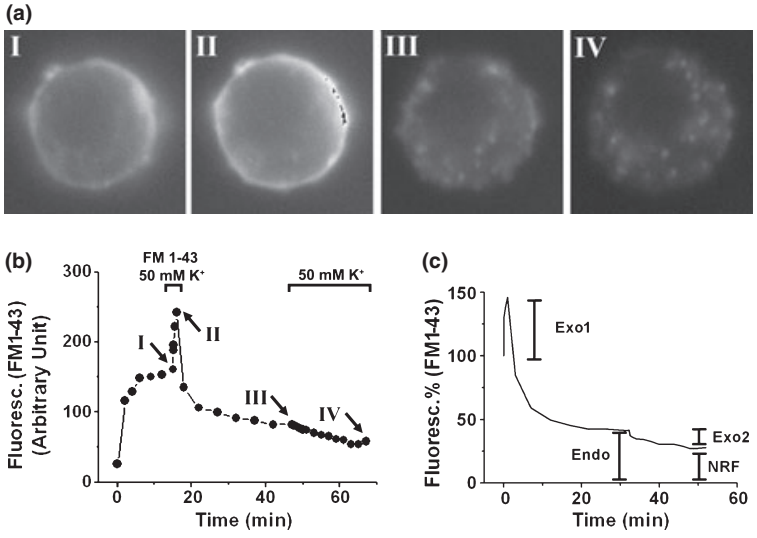

Figure 1 Evaluation of exocytosis, endocytosis and vesicle recycling during a single experiment: (a) Fluorescence images from one single cell obtained at the end of the following steps (see Materials and Methods): I. 15-min incubation in standard solution with FM 1-43. II. 60-s stimulus with 50 mM K^+, still in the presence of FM1-43. III. 30-min washout in standard solution without FM1-43. IV. 30-min application of 50 mM K^+ to induce exocytosis and the consequent distaining of internalized FM 1-43. (b) Time course of the spatially averaged fluorescence of the same cell represented in panel (a). The arrows indicate the end of the steps described earlier. (c) Time course of FM1-43-associated fluorescence normalized to the values obtained at the end of FM1-43 incubation period (point I at b). The curve is the average of 14 individual experiments similar to the one showed in (b). The brackets indicate the different parameters measured in our experiments: Exo1 (exocytosis provoked by 60-s depolarization); Endo (total membrane internalized by endocytosis); Exo2 (releasable fraction of internalized membrane); and NRF (non-releasable fraction of internalized membrane). The images represented in (a) are raw, and no subtraction was performed. Non-specific FM1-43 staining was subtracted from the experimental values represented in figures (b and c), as well as in all the other figures of this work.

previously endocytosed membrane. This last step provided information about the recycling of internalized membrane to new releasable vesicles within the time frame of the experiment. There was also a certain amount of fluorescence remaining at the end of the second depolarization, which was an estimation of the non-releasable fraction (NRF) of internalized membrane. In a previous paper (Perez Bay *et al.* 2007), we performed the appropriate controls to validate our parameters of exocytosis, endocytosis and vesicle recycling. It should be mentioned that (i) Exo1, Endo and Exo2 were null when the depolarization to trigger Exo1 was not applied, meaning that these processes are consequence of stimulus-evoked exocytosis and not related to constitutive cycling; and (ii) there was not significant distaining of FM1-43 if the second depolarization was applied in nominal zero calcium concentration, implying that Exo2 is a real process associated with a Ca^{2+}-dependent fusion of FM1-43-containing vesicles.

Figure 1(c) represents the average of 14 individual experiments, each one normalized to the fluorescence values obtained at the end of FM1-43 incubation period (point I at b). The brackets indicate the different parameters measured in the experiments. All FM1-43 data in this work were expressed in this way, except for Figure 7(b), where the values during Exo2 were normalized to the end of FM1-43 washout (point III in Fig. 1b). Some experiments were conducted in the presence of specific inhibitors, which were applied in the following manner: bisindolylmaleimide (100 nM) was applied during the whole experiment, except for the second stimulus (ExoII); thapsigargin was applied 45 min before and up to the end of the first stimulus (Exo1); ryanodine, nitrendipine or ω-Agatoxin IVA was applied 15 min before and up to the end of the first stimulus. We also performed experiments using nicotine or carbachol to trigger Exo1 instead of high K^+, but the general experimental scheme remained always the same.

To study the internalization of 70 kD tetramethylrhodamine (TMR) dextran, cells were incubated for 15 min with 50 μM 70 kD TMR dextran, stimulated for 30 s still in the presence of the dye, washed out for 30 min and finally stimulated again for 30 min. Fluorescence images (512 × 512 pixels, resolution 0.23 μm per pixel) were obtained at the end of this procedure with an Olympus FV 300 confocal microscope with a 60× water-immersion objective (confocal aperture fixed at 150 μm). A neon laser (543 nm) was used to excite the dye.

Cytosolic calcium measurements

To follow the relative cytosolic Ca^{2+} changes, cells were incubated with 5 μM Fluo-4 AM at 37 °C during 45 min in the presence of 0.04% pluronic acid and washed for 1 min at the same temperature before starting the experiment. The epifluorescence set-up and filter block were the same as in FM1-43 experiments. Calcium relative changes were expressed as $\Delta F/F$, where F is the spatially averaged fluorescence of the cell before stimulation and ΔF represents the increase in fluorescence induced by the stimulus.

Immunofluorescence experiments

Chromaffin cells were subjected to the protocol described above (Exo1 was induced with high K^+, 30 s) to stain the NRF with fixable FM1-43. Immediately after the end of the protocol, cells were washed two times with phosphate-buffered saline (PBS), fixed with 2% paraformaldehyde in PBS for 10 min, washed twice with PBS, permeabilized with 0.2% Triton X-100 in PBS (7 min), blocked with normal goat serum (5% in PBS) for 40 min and washed three times with PBS. Cells were then exposed for 90 min to rabbit anti-giantin antibody (1 : 400; Covance, Princeton, NJ, USA), mouse anti-transferrin receptor antibody (1 : 300; Zymed, Carlsbad, CA, USA) or mouse monoclonal antibody H4A3 to Lamp1 (1 : 1000; Developmental Studies Hybridoma Bank (NICHD)). After washing three times with PBS, the cells were incubated for 30 min with alexa Fluor 405-conjugated with anti-mouse or anti-rabbit secondary antibodies (Molecular Probes, Carlsbad, CA, USA), respectively, and mounted on glass slides. Samples were examined in a Leica TCS SP2 confocal microscope with a 63× oil-immersion objective (1.4 NA).

Whole-cell patch clamp and membrane capacitance measurements

Conventional whole-cell recordings were performed as detailed previously (Alvarez *et al.* 2008). The patch-clamp set-up comprised a patch-clamp amplifier (Model EPC7; LIST-MEDICAL, Darmstadt, Germany), a data acquisition interface (DigiData 1200 series; Axon Instruments Inc, Foster City, CA, USA) and a personal computer. The voltage applied to the cell at basal conditions was composed of the sum of a sinusoidal voltage (390 Hz, 80 mV peak to peak) and a holding potential of −80 mV. We found that this relatively low sinusoidal wave frequency does not increase our capacitance measurements noise (in rms) respect 780 Hz. During the depolarizing voltage pulses, the sinusoidal pattern was suspended. The holding potentials were not corrected for junction potentials (Neher 1992). The cells were considered 'leaky' and discarded when the leak current measured at the normal holding potential of −80 mV was bigger than −30 pA. Cell membrane capacitance was measured with a software phase-sensitive detector (jClamp; Sci Soft, Branford, CT, USA). The data were filtered at 3 kHz.

Chemicals and drugs

Bovine serum albumin, poly-L-lysine, cytosine-1-β-arabinofuranoside, papain, carbachol, thapsigargin and ryanodine were obtained from Sigma (St Louis, MO, USA); Dulbecco's modified Eagle's medium, foetal calf serum, gentamicin and penicillin/streptomycin from GIBCO (Carlsbad, CA, USA); fluorescent indicators (FM 1-43, Fluo-4 AM and TMR dextrans) were purchased at Molecular Probes (Portland, OR, USA); nitrendipine was obtained from Tocris Bioscience (Park Ellsville, MO, USA), ω-Agatoxin IVA from Alomone Labs (Har Hotzvim Hi-Tech Park, Jerusalem, Israel) and nicotine and bisindolylmaleimide-1 from Calbiochem (San Diego, CA, USA).

Data analysis and statistics

Images from FM1-43 experiments were quantified with the Axon Imaging Workbench 2.1 program (Axon Instruments) by measuring the spatially averaged fluorescence of the whole cell at the equatorial section and subtracting the background fluorescence (quantified from the surrounding field). Exo2 was obtained from the asymptote of a double exponential fitting performed on the experimental distaining curve. There was <10% of difference between the Exo2 estimated with this methodology and the value obtained by simple difference between the previous and the last measured points of the distaining curve (Perez Bay *et al.* 2007). The sizes of the fluorescent spots associated with NRF (Fig. 6c) were estimated with Image Pro software (Media Cibernetics, Silver Spring, MD, USA) as the full width at half-maximum (FWHM) of the spots' fluorescence profiles fitted to a Gauss function (Perez Bay *et al.* 2007). The Ca^{2+} transient decay rate was quantified as $T_{50\%}$, i.e. the time elapsed from the peak of the transient to 50% of the peak value. Linear and non-linear fittings were carried out with Origin's (Microcal Sotware Inc, Northhampton, MA, USA) specific tools. Data are expressed as mean values ± standard error. We used Student's '*t*' test for comparisons between independent data samples and paired '*t*' test for paired data samples.

Results

A transient excess retrieval process in mouse chromaffin cells

The main goal of this work was to study the fate of the membrane internalized during excess retrieval. Therefore, we had to find first an experimental condition that allowed us to detect excess retrieval with FM1-43. To this end, we varied the length of high K^+ depolarizations to obtain Exo1 of different magnitudes (Fig. 2a), and then we compared Exo1 vs. Endo for each condition (for definitions and validations of Exo1, Endo, Exo2 and NRF see Materials and Methods; Perez Bay *et al.* 2007). Exo1 and Endo were statistically identical for stimulus durations equal to or longer than 60 s, but for 30- and 15-s stimuli, Endo almost duplicated Exo1. We defined the excess retrieval membrane pool or ERMP as the difference Endo–Exo1, which is the amount of membrane internalized by endocytosis that exceeded the previous exocytosis. For the single experiment of Figure 2(b), Exo1 and Endo were 22 and 32%, respectively, so ERMP was 10%. The averaged value of ERMP obtained for 30 and 15 s stimuli were 16 ± 2% (n = 39) and 12 ± 3% (n = 17) respectively.

According our protocol design, the FM1-43 was removed at the end of the stimulus, and in consequence, the measured endocytosis had to progress during the stimulation. Therefore, our results are in agreement with previous data obtained by capacitance measurements on bovine chromaffin cells, showing that rapid endocytosis leading to excess retrieval is completed in approx. 30 s (Artalejo *et al.* 1995, 1996, Engisch & Nowycky 1998). To evaluate this issue, we studied the time evolution of membrane capacitance of mouse chromaffin cells in response to a stimulus that is expected to induce excess retrieval according to our FM1-43 data. Using the patch-clamp/whole-cell technique, we measured the change in membrane capacitance provoked by a 15-s depolarization square pulse from a holding of −80 to −10 mV. An individual example of these experiments is represented in Figure 2(d). We added a record representing the capacitance changes obtained in response to a 1000-ms depolarization pulse (Fig. 2e), which gives a more complete representation of endocytosis temporal kinetics. Both records (d and e) show that excess retrieval (the peak of excess retrieval is represented by double arrows) was produced owing to a typical rapid endocytosis event which was completed in no more than 30 s, similar to the pattern described in bovine cells (Artalejo *et al.* 1995). In summary, the application of a 15-s depolarization pulse induced a net capacitance decrease of 639 ± 176 $\Delta F/F$ (n = 5), measured from the pre-stimulus capacitance level to the minimum value after the stimulus (represented by the double arrow in the individual example of Fig. 2d). Measured in that way, this value represents specifically the ERMP. If we express our individual experimental values as percentages of initial whole-cell capacitance, they represent a 10 ± 3% decrease in plasma membrane surface. This value is similar to the ERMP measured with FM1-43 after 15-s high K^+ depolarizations. These results together indicate that the excess retrieval revealed by our experimental approach (with FM1-43) is the consequence of a rapid endocytosis process, as the one defined

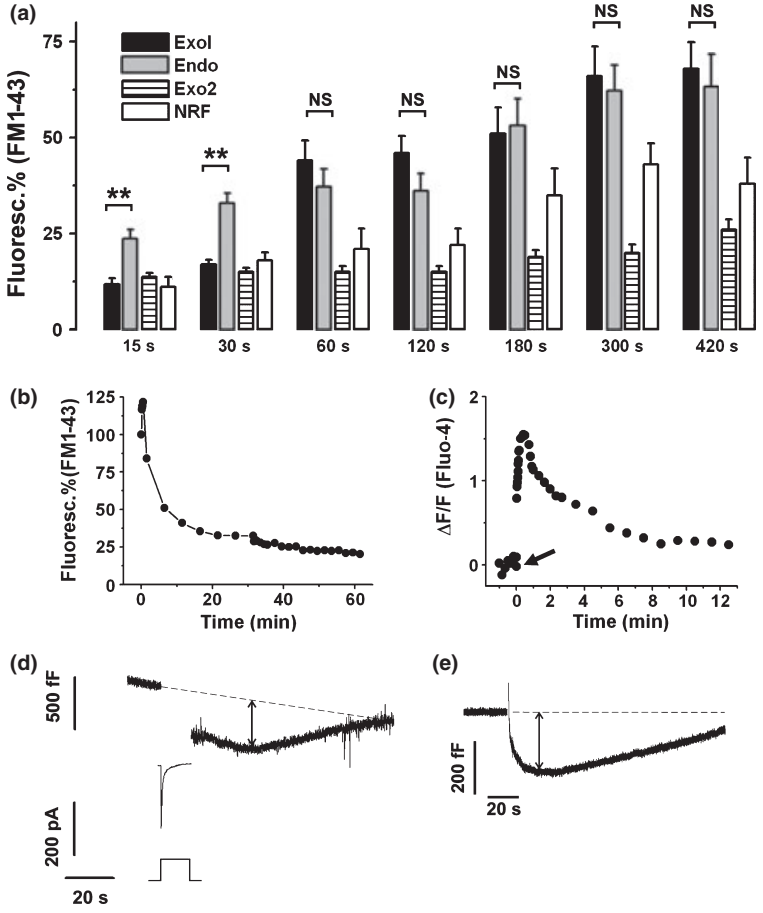

Figure 2 Identification of excess retrieval with FM1-43: (a) The bar diagram represents Exo1, Endo, Exo2 and NRF in cells where Exo1 was induced by the application of 50 mM K^+ during 15, 30, 60, 120, 180, 300 or 420 s (the number of cells was 17, 39, 14, 18, 26, 15 and 14 respectively). Note that Endo was statistically identical to Exo1 for all stimulation lengths, with the exception of 15 and 30-s stimulus. $^{**}P < 0.001$; NS means no significant statistical difference. (b) Time course of the fluorescence associated with FM1-43 from one single cell in which Exo1 was induced by a 30-s high K^+ depolarization. (c) Cytosolic calcium time course (expressed as $\Delta F/F$) from a single cell loaded with the calcium indicator Fluo-4 AM and stimulated like in (b). (d) Experimental record showing the change in membrane capacitance (top) of one cell before and after the application of a 15-s depolarization square pulse (bottom), from −80 mV holding potential to −10 mV. The Ca^{2+} current activated by the depolarizing pulse is also represented (middle). (e) Membrane capacitance time course of one cell before and after the application of a 1000-ms depolarization square pulse, from −80 mV holding potential to 0 mV. The Ca^{2+} current associated with this experiment (150 pA of amplitude) is not represented because of the time scale of the figure. The dotted lines in (d) and (e) are linear extrapolations of the last 5 s of the capacitance record baselines obtained previously to the application of the depolarization pulse. The double arrow indicates the peak of the excess retrieval process.

kinetically by capacitance measurements. It is important to note that only approx. 50% of the membrane internalized during 15- or 30-s depolarizations becomes releasable at the time that Exo2 is evoked (Fig. 2a), while the other half remains as a non-releasable fraction. Therefore, rapid endocytosis leading to excess retrieval seems to be a complex process, involving at least two intracellular membrane pathways.

Because excess retrieval was maximal after the application of a 30-s depolarization, we therefore used this condition as our control stimulus to study this process. Figure 2(b,c) shows examples of FM1-43 fluorescence and calcium signal time courses, both induced by 30-s high K^+ depolarizations. The calcium transient reached the peak (Table 1) at 18 ± 1.5 s and remained high for a long time (Fig. 2c, also note the $T_{50\%}$ for control cells in Table 1), so it possibly could continue inducing exocytosis and/or affecting endocytosis even after FM1-43 removal. To study this issue, the 30-s stimulus was applied in the same way as in Figure 2(b), but FM1-43 was kept in standard (normal K^+) solution for additional 30 s after the end of the depolarization. Application of the dye for this extra period allowed us to assess exocytosis and endocytosis occurring after the end

Table 1 Calcium transient parameters and excess retrieval

Treatment	Ca^{2+} peak ($\Delta F/F$)	$T_{50\%}$ (s)	Endo–Exo1 (%)
Control	2.2 ± 0.3 (34)	181 ± 25	16.0 ± 2.3 (39)
Nitre	0.33 ± 0.06 (8)*	485 ± 80*	−0.8 ± 2.5 (12)*
AGA	1.9 ± 0.3 (15)	129 ± 35	12.0 ± 2.6 (12)
Ryan	1.1 ± 0.2 (20)*	105 ± 27*	7.0 ± 2.7 (16)*
Thaps	1.1 ± 0.3 (15)*	102 ± 22*	0.8 ± 2.3 (13)*

Nitre, Nitrendipine; AGA, Ω-Agatoxin IVA; Ryan, Ryanodine; Thaps, Thapsigargin. Nitre, AGA, Ryan y Thaps were compared vs. control, with a significance level of 0.05. In all conditions, Exo1 was induced by the application of 50 mM K^+ during 30 s. Excess retrieval was calculated as Endo–Exo1. The number of cells for each group is represented between parentheses. * $P<0.05$

of the stimulus. Figure 3(a) represents the FM1-43 fluorescence time course of an individual cell under that experimental condition. After the end of the stimulus, there was an additional increase in fluorescence, representative of membrane fusion (Fig. 3a, inset). These experiments are summarized in Figure 3(b). The total developed exocytosis (during 30-s stimulus + additional 30-s period) was not different than Endo (n = 24). We interpret these results as follows: during the 30-s high K^+ application, endocytosis surpasses exocytosis transiently provoking excess retrieval (Endo > Exo1, $P < 0.05$), but asynchronous exocytosis after the end of depolarization yields a final balance between the total amounts of fused and retrieved membrane. The experiment represented in Figure 3(a) suggests the possibility that asynchronous exocytosis could continue even beyond the 30 s after the end of the depolarization. Therefore, we extended the period with FM1-43 after the stimulus to 150 s (Fig. 3c,d). These experiments revealed some further increase, but total exocytosis was not significantly different than endocytosis (Fig. 3d, n = 15), showing again that after the high

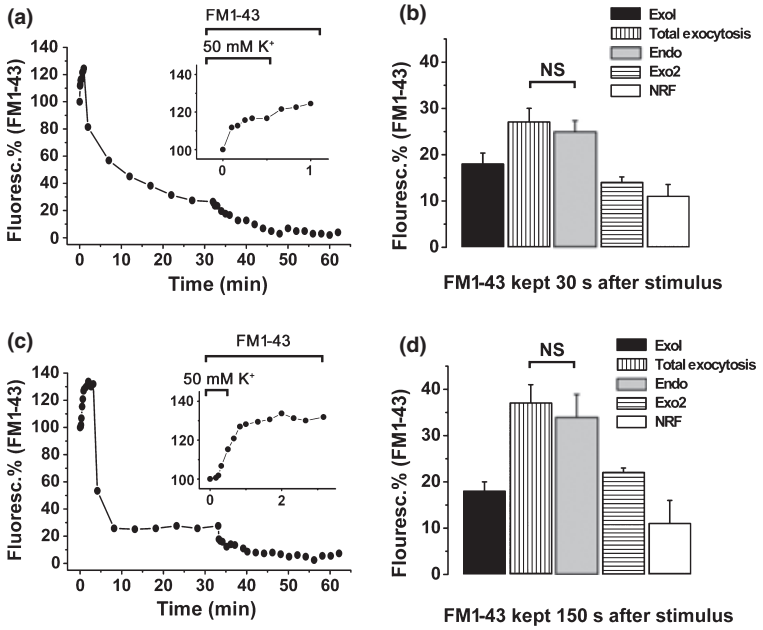

Figure 3 Excess retrieval is balanced by asynchronous exocytosis: (a) Time course of FM1-43 associated fluorescence from a single cell. The protocol was similar to the one applied in the experiment of Figure 2(b), but the cell was exposed to FM1-43 (in standard solution) for additional 30 s after the end of the 30-s stimulus. The inset represents this complete 60-s period in the presence of FM1-43. (Note that exocytosis continues after the end of stimulus.) The bar diagram (b) summarizes the results of this type of experiments (n = 24). 'Total Exocytosis' represents the sum of Exo1 plus asynchronous exocytosis produced during the extra 30-s FM1-43 application. The experiment represented in (c) was similar to the one in (a), but FM1-43 was maintained for additional 150 s after stimulus. The bar diagram in (d) summarizes the results of the type of experiments represented in panel (c) (n = 15). Note that in the two conditions represented in this figure total exocytosis was not different than Endo. NS means no difference between samples.

K^+ depolarization, both processes are finally balanced. The asynchronous exocytosis unmasked by these experiments is probably equivalent to the 'recovery after excess retrieval' process described by capacitance measurements on bovine chromaffin cells (Artalejo *et al.* 1995). It is important to note that a similar phenomenon of membrane capacitance recovery was observed by us on mouse cells (Fig. 2d,e).

We next wondered whether excess retrieval could be also induced by close-to-physiological stimuli, like application of cholinergic agonists. Nicotine (200 μM, during 30 s) induced Exo1 of $14 \pm 1\%$, which was slightly but significantly exceeded by Endo (Fig. 4a, $P < 0.05$, $n = 33$). In this experimental condition, the Ca^{2+} transients had a peak of 1 ± 0.2 $\Delta F/F$ ($n = 19$) at 10 ± 1 s after the beginning of stimulus (Fig. 4c shows a typical record). Carbachol was more effective than nicotine to provoke excess retrieval (Fig. 4b, $P < 0.001$, $n = 26$), evoking Ca^{2+} transients with a peak of 1.3 ± 0.2 $\Delta F/F$ ($n = 19$) at 10 ± 1 s (see Fig. 4d for an example). From the experiments performed with cholinergic agonists and high K^+ depolarizations, it seems that ERMP increases in the same direction (nicotine < carbachol < high K^+) as Ca^{2+} signals. The calcium dependence of ERMP will be studied in the next section.

Excess retrieval is regulated by calcium

To investigate the relationship between excess retrieval and the intracellular calcium signal, we studied, in independent experiments, the effect of different external calcium concentrations ($[Ca^{2+}]_o$) on the amplitude of Ca^{2+} transients and on ERMP. The $[Ca^{2+}]_o$ was modified only during the stimulus to induce Exo1 or the Ca^{2+} transient, but during the rest of the experiment, $[Ca^{2+}]_o$ was kept constant at 2 mM. Figure 5(a) shows the averaged values of Exo1, Endo, Exo2 and NRF, and Figure 5(b) displays original examples of fluorescence (%) FM1-43 signals. There was a consistent and significant increase in Ca^{2+} transients' amplitudes, Exo1, Endo and NRF with $[Ca^{2+}]_o$ ($P < 0.05$). Because Endo followed a steeper calcium dependence than Exo1, ERMP augmented with increasing $[Ca^{2+}]_o$. The averaged values of ERMP at each $[Ca^{2+}]_o$ were plotted versus the averaged values of the calcium transient peak (open circles, Fig. 5c). We found a highly significant correlation between these two variables ($R > 0.9527$, $P < 0.005$). On the other hand, no correlation was found between ERMP and Exo1 (Figure S1 Supporting information).

We next analysed the Ca^{2+} sources that might contribute to the control of excess retrieval. It was recently described that L-type Ca^{2+} channels are preferentially coupled to rapid endocytosis in bovine chromaffin cells (Rosa *et al.* 2007). In our preparation, we found that the L-type Ca^{2+} channel blocker nitrendipine (20 μM) reduced markedly the calcium transient peak and totally abolished the ERMP (Figure S2 Supporting information, Table 1), whereas the P/Q-type Ca^{2+} channel inhibitor ω-agatoxin IVA (200 nm) did not produce any effect (Table 1). We demonstrated before that our chromaffin cell preparation lacks a significant N-type current contribution (Alvarez *et al.*

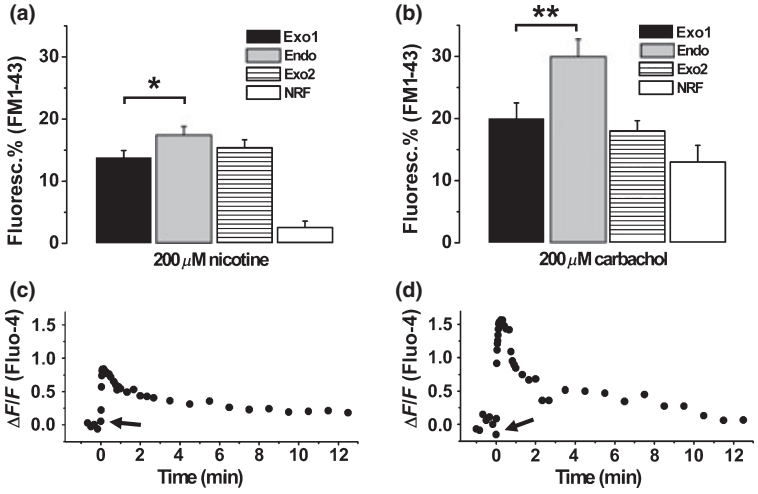

Figure 4 Excess retrieval is triggered by cholinergic stimulation: The bar diagrams represent the average values of Exo1, Endo, Exo2 and NRF, obtained from experiments in which Exo1 was induced by the application of 200 μM nicotine (a) or 200 μM carbachol (b) during 30 s. Excess retrieval was generated under both conditions, but it was more evident in (b); (c and d) are examples of Ca^{2+} transients measured in single cells loaded with Fluo-4 AM and stimulated during 30 s with 200 μM nicotine or 200 μM carbachol respectively. *$P < 0.05$; **$P < 0.001$.

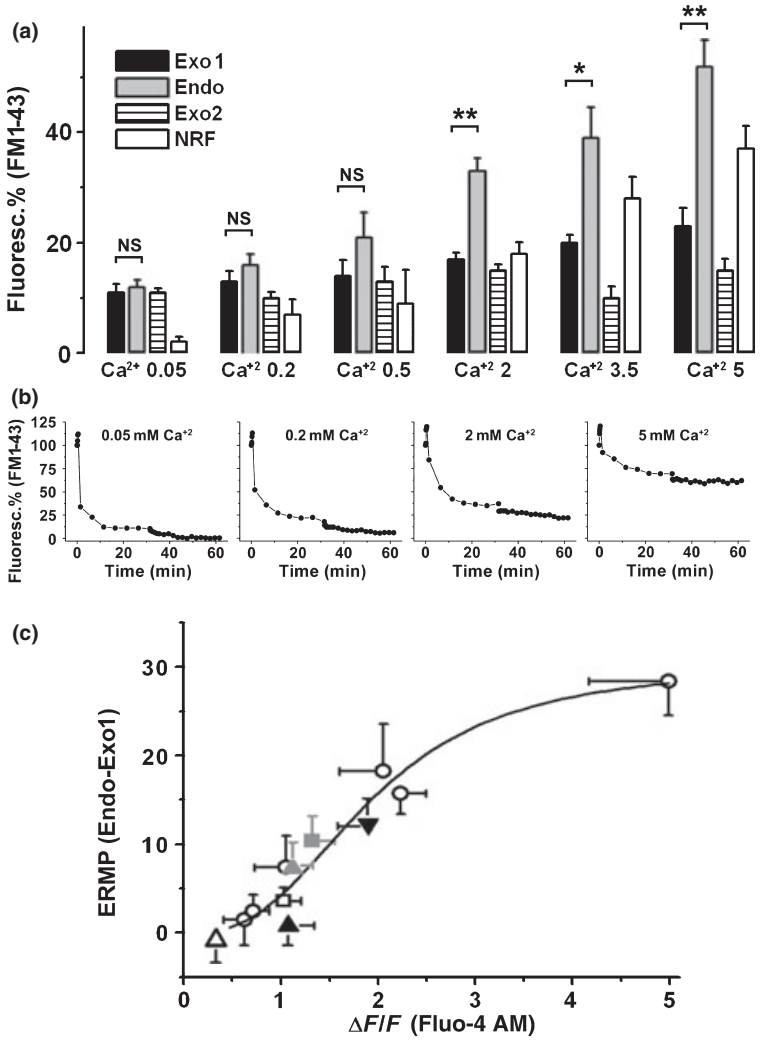

Figure 5 Activation of excess retrieval depends on calcium: (a) The bar diagram represents the average values of Exo1, Endo, Exo2 and NRF obtained from experiments where the stimulus to induce Exo1 was the application of 50 mM K^+ during 30 s at different $[Ca^{2+}]_o$, 0.05, 0.2, 0.5, 2, 3.5 and 5 mM (the number of cells was 4, 15, 8, 39, 9 and 13 respectively). Solutions did not contain EGTA, except the solution containing 0.05 mM calcium, which was prepared with 950 μM Ca^{2+} plus 900 μM EGTA. (b) Representative examples of the time course of the fluorescence (%) associated with FM1-43, obtained in single cells stimulated with 50 mM K^+ during 30 s, in the presence of 0.05, 0.2, 2 and 5 mM $[Ca^{2+}]_o$. (c) The averaged ERMP (Endo–Exo1) for each condition was plotted against the averaged calcium transient peak and fitted to a Hill Equation ($Y = Y_{max} \frac{x^{n_b}}{K^{n_b}+x^{n_b}}$). This regression is represented by the black line (K = 1.94 ± 0.26; Y_{max} = 30.4 ± 3.7, n_b = 2.73 ± 0.58, R = 0.97308; n = 11). The open circles represent the values obtained from cells stimulated with high K^+ at different calcium concentrations (the number of calcium measurements in individual independent experiments with 0.05, 0.2, 0.5, 2, 3.5 and 5 mM $[Ca^{2+}]_o$ was 4, 14, 10, 34, 11 and 16 respectively); white and grey squares represent experiments in which Exo1 was induced by the application of 200 μM nicotine or 200 μM carbachol respectively (see Fig. 4); white, black, grey and inverted triangles represent experiments performed with 20 μM nitrendipine, 1 μM thapsigargin, 100 μM ryanodine and 100 nM ω-agatoxin IVA respectively. * $P < 0.05$; ** $P < 0.001$.

2008), so we did not apply specific blockers for these channels. Next, to evaluate the possible contribution of Ca^{2+} release from endoplasmic reticulum (ZhuGe *et al.* 2006), we applied 100 μM ryanodine. This treatment reduced significantly both the Ca^{2+} transient peak and ERMP (Table 1). Moreover, the pre-treatment with thapsigargin (1 μM, 45 min), to induce endoplasmic reticulum Ca^{2+} depletion, also decreased markedly the Ca^{2+} transient peak and abolished ERMP (Table 1). These results together show that not only L-type Ca^{2+} channels but also the endoplasmic reticulum participate in the cytosolic calcium signal, contributing together to trigger excess retrieval under our stimulation conditions.

The experiments described above support the idea that the endocytic process responsible for excess retrieval is strongly regulated by cytosolic Ca^{2+}, inde-

pendently of the well-known effect of this cation on exocytosis (Fig. 5c and Figure S1 Supporting information). The averaged ERMP obtained in experiments performed with ryanodine (grey triangle), thapsigargin (black triangle), nitrendipine (white triangle), ω-agatoxin IVA (inverted triangle), nicotine (white square) and carbachol (grey square) were plotted versus the corresponding averaged calcium transient peaks, together with the results of the experiments at various Ca^{2+} concentrations (open circles), and fitted to a Hill equation (Fig. 5c, black continuous line, $R > 0.9730$, $n = 11$). We judged that this model was a good representation of excess retrieval Ca^{2+} dependency, in first place because we expect saturation, and secondly because it considers the existence of a threshold for excess retrieval activation (Smith & Neher 1997, Engisch & Nowycky 1998).

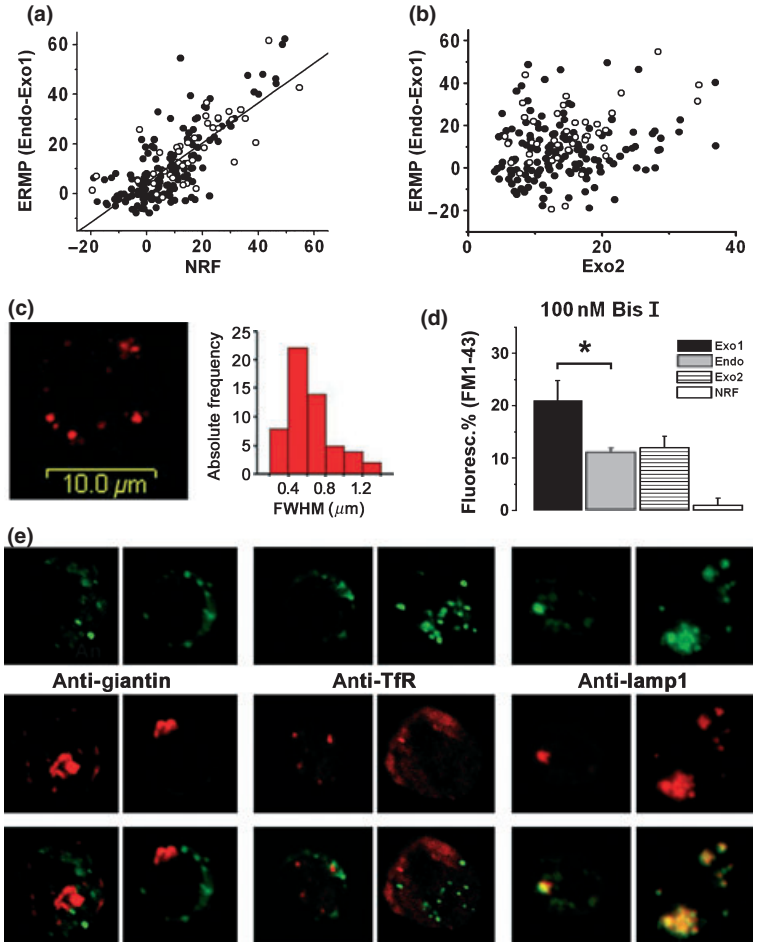

Figure 6 Excess retrieval is associated with the formation of NRF: (a) ERMP (Endo–Exo1) values from individual experiments were plotted against NRF. The linear regression is represented by the straight black line ($R > 0.7619$; $n = 189$). (b) ERMP was plotted against Exo2 ($R = 0.2298$; $n = 189$). In both figures (a and b), opened circles represent observations obtained in our standard experimental condition (50 mM K^+, 2 mM Ca^{2+}), and filled circles correspond to experiments performed in all the other conditions represented in Figure 5(c). (c) Spatial distribution of NRF. Confocal images were obtained at the end of experiments performed in the presence of 50 μM 70 kD TMR dextrans. The image (on the left) was selected from a total of 10 cells, all of them showing a similar patter. For more details, see Materials and Methods and Results. The histogram (right) represents the size (measured as FWHM, see Materials and Methods) distribution of fluorescent spots ($n = 55$). (d) Bar diagram representing Exo1 (induced by 50 mM K^+ during 30 s), Endo, Exo2 and NRF for experiments ($n = 12$) performed in the presence of 100 nM bisindolylmaleimide-1 (Bis I). *$P < 0.02$. (e) Confocal images of chromaffin cells, fixed at the end of our standard protocol and immunostained with primary antibodies against specific cellular organelles plus 405 alexa-conjugated anti-rabbit or anti-mouse secondary antibodies (for details, see Materials and Methods). The upper row shows fluorescent images associated with NRF, labelled with fixable FM1-43. The row at the middle shows the spatial distribution of anti-giantin antibodies (two columns at the left), anti-transferrin receptor antibodies (two columns in the middle) and anti-Lamp1 antibodies (two columns at the right). The bottom row shows the merged images of the first two rows. Note that NRF only colocalizes with the compartment stained with anti-Lamp1 antibodies.

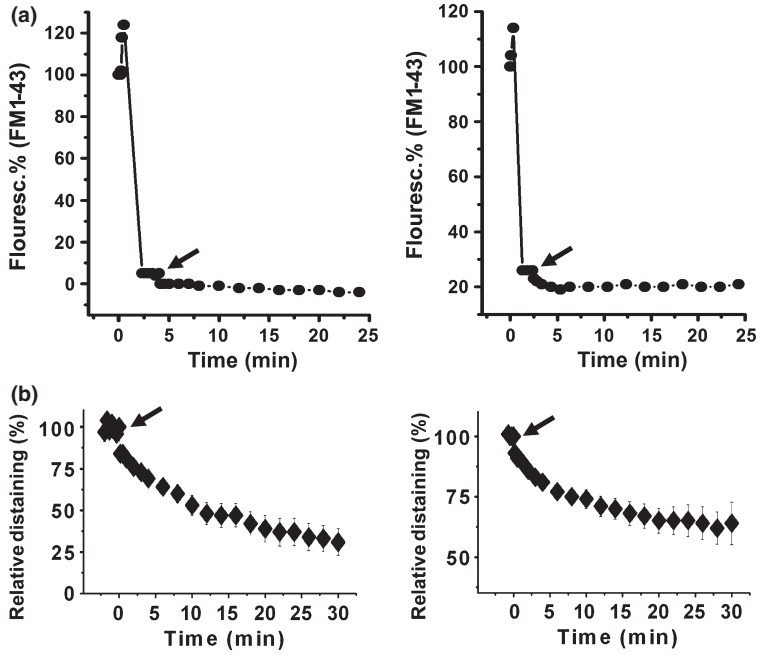

Figure 7 The releasable fraction Exo2 is generated in a short time period: (a) Two individual experiments showing the time course of FM1-43-associated fluorescence. The washout of FM1-43 was shortened to 3.5 min (left) or 2 min (right) by applying 1 mM ADVASEP-7 during the first minute after Exo1. With this procedure, the fluorescence reached a stable plateau before the end of the washout (Perez Bay *et al.* 2007). The arrows indicate the start of the fluorescence distaining (induced by 50 mM K^+). (b) Averaged curves of fluorescence distaining for the type of experiments represented in (a) (left: 3.5 min washout, $n = 10$; right: 2 min washout, $n = 7$). For better visualization of the distaining curves, only the last points of the washout period are represented, and values were normalized to the end of the washout period.

To further study the calcium dependency of the endocytosis process involved in excess retrieval, we analysed its divalent cation specificity (Artalejo *et al.* 1995). We performed experiments replacing bath Ca^{+2} with equimolar Ba^{+2} during Exo1. The most notorious effects observed under this experimental condition were the complete lack of excess retrieval and the presence of a negligible NRF (Figure S3 Supporting information).

Excess retrieval generates a non-releasable fraction of membrane

Our results consistently indicate that the internalized membrane is driven through two different pathways, leading to the recovery of a releasable fraction of membrane (Exo2) and the formation of NRF respectively (see above in this paper; Perez Bay *et al.* 2007). Consequently, we wondered whether excess retrieval might be associated specifically with any of these two membrane fractions. At first sight it seems that ERMP follows a similar behaviour as NRF, along the different conditions tested (see Figs 5a, 6d and 4a, and Figures S3 and S5 Supporting information). To confirm that observation, we plotted these two variables (Fig. 6a) and observed an approximately linear relationship and a good correlation ($R > 0.7619$, $n = 189$). On the other hand, we did not find correlation between ERMP and Exo2 ($R = 0.2298$, $n = 189$, Fig. 6b). These results suggest that the process involving excess retrieval is associated with the internalization of NRF.

To study the endocytic mechanism responsible for NRF, we investigated the endocytosis and spatial localization of high-molecular-weight fluorescent dextrans. The cellular uptake of 70-kDa TMR dextrans was induced by the application of 50 mM K^+ during 30 s, then the dextrans were washed out from bath solution, and the cell was stimulated again (with high K^+) for 30 min (see Materials and Methods). Figure 6(c) (left) represents a typical example of a cell image obtained at the end of this process. The image shows several cytosolic fluorescent spots produced by dextran internalization, similar to the ones observed at the end of FM1-43 experiments (Fig. 1a). These endosomes were not formed by kiss and run, because 70-kDa dextrans are not allowed to permeate through small fusion pores (Fulop *et al.* 2005). Moreover, the fluorescent spots, estimated as FWHM (see Materials and Methods), were 0.63 ± 0.03 μm in size ($n = 55$, obtained from 10 cells, see Fig. 6c, right), similar to the vacuoles produced by bulk endocytosis in several systems (Holt *et al.* 2003, Perez Bay *et al.* 2007, Wu & Wu 2007).

To continue the identification of the cellular compartments associated with NRF, we used specific antibodies against the Golgi, early endosomes and lysosomes and studied the colocalization of these organelles with the NRF. Figure 6(e) shows confocal images of cells co-stained with fixable FM1-43 (to mark NRF) and anti-giantin, anti-transferrin receptor or anti-Lamp1 antibodies [markers of Golgi (Linstedt & Hauri 1993), early endosomes (Knight 2002, Maxfield & McGraw 2004), or lysosomes (Nie *et al.* 2003) respectively]. FM1-43 was applied according to our standard protocol, and antibodies were added after cell fixation and permeabilization at the end of experiments (see

Materials and Methods). We observed a clear colocalization between NRF and the lysosomal compartment, both appearing as punctuate structures (Fig. 6e, pair of columns on the right). Approximately 50% of the NRF spots colocalized with the lysosomal spots, whereas almost all Lamp1 spots (96%) colocalized with FM1-43. On the other hand, NRF did not colocalize with Golgi or early endosomes (Fig. 6e, two columns on the left and two columns on the middle). For negative controls without primary antibodies (see Figure S4 Supporting information).

The type of membrane retrieval is in part a consequence of the mode of vesicle fusion. It was shown that bovine chromaffin cells shift the exocytic mode from 'kiss and run' to 'full collapse' in a Ca^{2+} regulated manner (Fulop *et al.* 2005, Fulop & Smith 2006) through a mechanism involving PKC activation. Because during 'full collapse' the vesicle fuses completely in the membrane loosing its identity, it is expectable that membrane retrieval will proceed through clathrin-dependent or even bulk endocytosis pathways, generating endosomes that will not cycle rapidly to releasable vesicles. We have shown above that excess retrieval is a calcium-dependent phenomenon, not associated with rapid recovery of releasable vesicles but related to the formation of NRF. Therefore, we wonder whether NRF formation and excess retrieval could be affected by PKC inhibition. The PKC inhibitor bisindolylmaleimide-1 (100 nM) abolished completely excess retrieval in experiments where Exo1 was induced with a high K^+ depolarization (Fig. 6d) or by application of 200 μM nicotine (Figure S5 Supporting information). These results show that in our experimental conditions, an important fraction of endocytosis, which is responsible for excess retrieval, depends on PKC activity. It is also important to note that PKC inhibition completely abolished NRF formation (Fig. 6d and Figure S5 Supporting information), in agreement with the correlation observed between ERMP and NRF (Fig. 6a) and supporting our conclusions about the fate of ERMP.

A recycling pathway recovers releasable vesicles in a short time period

In the previous section, we showed that the ERMP internalized during rapid endocytosis is correlated with NRF. However, other authors proposed that rapid endocytosis was the first step of fast recycling of releasable vesicles (Elhamdani *et al.* 2006). Therefore, we studied how quickly the other portion of the membrane retrieved during 30-s high K^+ depolarizations was recycled to the releasable fraction Exo2. This can be tackled using a methodology introduced by us (Perez Bay *et al.* 2007) that allows to determine whether membrane recycling occurs in a period as short as 2 min. Briefly, we reduced the gap between the first stimulus (which triggered Exo1 and membrane retrieval) and the second stimulus (used to estimate the membrane cycling to releasable vesicles) by quickly washing out the extracellular FM1-43 with the scavenger ADVASEP-7. Figure 7(a) shows individual examples of this type of experiments, where the recycling to releasable vesicles was evaluated with a second depolarization applied 3.5 (left) or 2 min (right) after the first stimulus. Figure 7(b) shows the averaged curves of the fluorescence distaining obtained at those conditions. The second depolarization induced a clear decay in cell fluorescence, indicating the release of the FM1-43 trapped in previously internalized vesicles. Therefore, these experiments indicate that an important fraction of the membrane internalized by rapid endocytosis was cycled to releasable vesicles in <2 min after the end of the depolarization.

Discussion

Excess retrieval detection with FM1-43

After exocytosis, neurones and neuroendocrine cells have to retrieve the excess of plasma membrane and refill the depleted pools of vesicles (Rizzoli & Betz 2005). In a previous paper, we used a fluorescence assay with FM1-43 to study the recycling of internalized membrane after massive exocytosis in chromaffin cells (Perez Bay *et al.* 2007). We found that endocytosis compensated completely the previously induced exocytosis, but the type and intensity of stimulation provoked differences in the fate of internalized membrane: when exocytosis and endocytosis were ≤20% of plasma membrane, the internalized membrane recycled completely into new releasable vesicles in ≤2 min, but when exocytosis and endocytosis were larger, an additional non-releasable fraction was formed.

In the present work, we exploited the advantages of our experimental approach to study the fate of the membrane internalized by excess retrieval, which cannot be done by capacitance measurements. Excess retrieval was reliably reproduced in our preparation, showing a time evolution (Figs 2d,e and 3) similar to previous observations on bovine cells (Artalejo *et al.* 1995, Engisch & Nowycky 1998, Nucifora & Fox 1999). Our standard stimulus (high K^+ during 30 s) induced exocytosis and endocytosis equivalent to 17 and 32% of plasma membrane, respectively, generating an ERMP of 15% at the end of the depolarization. The total magnitudes of rapid endocytosis provoking excess retrieval reported by other authors (Artalejo *et al.* 1995, Smith & Neher 1997, Engisch & Nowycky 1998) were somewhat smaller than our estimation, but we should consider the differences in experimental conditions, stimulation protocols and cell types. In addition,

capacitance measurements (which was the technique used in those previous studies) may underestimate endocytosis because of its overlapping with exocytosis (Nucifora & Fox 1998). A parameter not affected by exocytosis–endocytosis overlapping is ERMP: when we approximated the stimuli conditions applied in FM1-43 experiments to voltage-clamp experiments, we obtained similar estimations for ERMP with both methodologies.

Excess retrieval is a transient event triggered by calcium

In our experiments, we measure the cumulative endocytosis until the moment that FM1-43 is removed from the bath. When FM1-43 was removed at the end of the 30-s high K^+ pulse, endocytosis was larger than exocytosis (Fig. 2). However, maintenance of FM1-43 after the end of the stimulus uncovered an asynchronous exocytosis process that balanced completely the effect of excess retrieval in < 30 s (Fig. 3), thus evidencing the transient nature of excess retrieval. An equivalent process, named 'recovery after excess retrieval', was also revealed by capacitance measurements (Artalejo *et al.* 1996, Engisch & Nowycky 1998, Neher & Zucker 1993; see also Fig. 2d,e in this work). To our knowledge, the mechanism underlying this process is still unknown. However, as our results showed that the cytosolic Ca^{2+} signal decreased with a very slow rate (Table 1, Fig. 2), it is reasonable to speculate that this process could be triggered simply by the residual Ca^{2+} remaining after the end of stimulus. In fact, 15 s after the end of our standard stimulus (i.e. during asynchronous exocytosis), the Ca^{2+} signal was still approximately at the 90% of the peak (Fig. 2c). More experiments will be needed to fully understand the regulation of this mechanism.

According to our data, excess retrieval is controlled by Ca^{2+} coming from extracellular and intracellular sources, is insensitive to Ba^{2+} and sensitive to PKC inhibition and is independent of previous exocytosis amplitude (Fig. 5; Figures S3 and S1 Supporting information). We found a clear correlation between ERMP and the calcium signal induced by different stimuli and from different Ca^{2+} sources (Fig. 5c). Previous publications reported that calcium entry had to exceed a certain threshold to activate excess retrieval (Smith & Neher 1997, Engisch & Nowycky 1998), but they failed to find a continuous relationship, as if excess retrieval was a sort of 'all or non' process. Our results are in agreement with the presence of a threshold, because ERMP became significant at $\Delta F/F$ values bigger than 1 (Fig. 5c). However, we described for the first time a continuous and saturable dependency between ERMP and cytosolic Ca^{2+} signal (Fig. 5c).

The blocking of L-type Ca^{2+} channels suppressed excess retrieval, in agreement with the results obtained by Rosa *et al.* (2007) in bovine cells. In a novel contribution, we also inhibited excess retrieval by preventing the release of Ca^{2+} from the endoplasmic reticulum with ryanodine or thapsigargin (Table 1). Therefore, our results support that excess retrieval is actually controlled by the concerted contribution of extracellular and intracellular Ca^{2+} sources. Interestingly, it should be noted that nitrendipine reduced the peak of the calcium signal in 86%, thapsigargin in 48% and ryanodine in 48%. These values are not merely additive, suggesting some type of synergism between extracellular and intracellular Ca^{2+} sources. A possible explanation is the activation of the Ca^{2+}-induced Ca^{2+} release mechanism (Fabiato 1983, Langer & Peskoff 1996). In fact, the presence of this sort of mechanism has been previously found in chromaffin cells (Alonso *et al.* 1999).

Excess retrieval is not associated with the cycling of releasable vesicles

Along this work, we found evidence indicating that the endocytosis process responsible of excess retrieval generates mainly non-releasable endosomes: ERMP correlated with NRF (Fig. 6a) but not with Exo2 (Fig. 6b), and NRF was absent or strongly reduced in all the experimental conditions lacking excess retrieval (Figs 5a and 6d, and Figures S3 and S5 Supporting information). In addition, for all types of stimuli (Figs 5, 2 and 4), an important amount of the internalized membrane was also cycled to the releasable fraction Exo2. Therefore, our data show that rapid endocytosis is a complex phenomena composed at least by two components, one associated with fast recycling of releasable membrane and another related to the generation of non-releasable endosomes (Perez Bay *et al.* 2007). This conclusion is in agreement with Engisch & Nowycky (1998) and with Smith & Neher (1997), who proposed the existence of two different rapid endocytosis mechanisms, responsible for excess and compensatory retrieval respectively.

The physiological function of excess retrieval remains elusive to researchers. It might be a restorative mechanism that internalizes the membrane overload accumulated by many previous small exocytic events (Neher & Zucker 1993). However, cell capacitance almost never remained at the new level achieved after excess retrieval but instead recovered to near the pre-stimulus level (Figs 2d,e, and 3; see also Artalejo *et al.* 1995, Engisch & Nowycky 1998). In addition, Engisch and Nowycky found that excess retrieval does not correlate with the amount of previously accumulated exocytosis (Artalejo *et al.* 1995, Engisch & Nowycky 1998). We suggest as alternative hypothesis that excess retrieval is a mechanism triggered by a strong cytosolic calcium increase that 'prelude' massive exocytosis and possible cata-

strophic cell swelling (Smith & Betz 1996, Rizzoli & Betz 2005). Under this hypothesis, the facts that endocytosis is transiently bigger than exocytosis and that asynchronous exocytosis finally compensates the transient membrane reduction could be simply interpreted as consequences of the balance between the temporal kinetics of both processes. The initial high Ca^{2+} increase provoked by the stimulus would surpass the threshold required for excess retrieval activation, and thereafter, the residual Ca^{2+} (Fig. 2c) after the stimulus would maintain a moderate exocytic activity, enough to keep the membrane surface at steady state.

Respect to the endocytic mechanism involved in excess retrieval, it cannot be a process associated with transient fusion/fission events, i.e. kiss and run or cavicapture, because this type of mechanism implies equivalent amounts of fused and retrieved membrane. In addition, kiss and run was classically associated with rapid recovery of releasable vesicles (Fulop *et al.* 2005), but we observed that ERMP was related to the formation of NRF. Possible mechanisms responsible for excess retrieval could be either clathrin-dependent endocytosis or bulk endocytosis. We have shown that NRF was mainly concentrated in long-lasting 0.6-μm endosomes, and it was specifically labelled by 70-kD dextrans (Fig. 6). In addition, in a previous work, we demonstrated the NRF was completely blocked by a phosphatidylinositol-3-phosphate kinase inhibitor (Perez Bay *et al.* 2007). These characteristics suggest that bulk endocytosis would be the predominant mechanism involved in NRF generation (Holt *et al.* 2003, Perez Bay *et al.* 2007, Clayton *et al.* 2008). Bulk endocytosis is triggered by strong stimulation, it develops in few seconds (probably activated by the same Ca^{2+} signal that evokes exocytosis) and involves the invagination of large areas of plasma membrane and formation of long-lasting vacuoles ranging from 0.5 to more than one micron in size (Clayton *et al.* 2007, 2008, Wu & Wu 2007). Similarly, excess retrieval is triggered by strong stimuli provoking significant cytosolic Ca^{2+} increase (Figs 2 and 5), it develops in few seconds (Fig. 2d,e; Engisch & Nowycky 1998) and is also associated with the formation of non-releasable approx. 0.6-μm endosomes suitable to be labelled by 70-kD dextrans (Fig. 6c).

To study the subcellular identity of NRF, we analysed the colocalization of this membrane pool with antibodies against specific organelle markers. Our results indicate that NRF colocalize with the lysosomal marker Lamp1, but not with the Golgi's marker giantin or the transferrin receptor pathway. The fact that NRF did not colocalize with transferrin receptors suggests that NRF does not fuse with early endosomes after internalization and is directed to the lysosomes without intercepting these compartments. A possible pathway by which the membrane reaches the lysosomes might be the one linked to pinocytosis, in which the internalized membrane fuses directly to late endosomes (Holt *et al.* 2003, Perret *et al.* 2005). Indeed, other authors, based on morphological evidence, have previously suggested that part of the membrane internalized after strong stimulation fuses to the lysosome compartment (Phillips *et al.* 1983, Patzak & Winkler 1986). A consequence of this hypothesis is that under conditions of intense exocytosis, a fraction of the releasable pool of vesicles will not recycle directly and will have to be recovered '*de novo*'.

In conclusion, the application of a 15- to 30-s depolarization triggers a fast endocytic mechanism responsible for excess retrieval (Fig. 2). Although an important portion of the internalized membrane recycles to a newly formed releasable fraction in a period consistent with the temporal evolution of rapid endocytosis, ERMP is related to the formation of non-releasable endosomes.

Conflicts of interest

There are not conflicts of interest with any person or institution.

We are especially grateful to Dr. Enrique Rodríguez-Boulan for helping us with the inmunolocalizations and for reading and criticizing our manuscript. We also want to thank to Drs Lidia Szczupak and Osvaldo Uchitel for the critical reading of our manuscript. This work was supported by grants PICT 05-11661 from Agencia Nacional de Promoción Científica y Tecnológica (Argentina), UBACyT X082 and UBACyT 461 from Universidad de Buenos Aires, and PIP 5847 from CONICET (Argentina).

References

Alonso, M.T., Barrero, M.J., Michelena, P., Carnicero, E., Cuchillo, I., Garcia, A.G., Garcia-Sancho, J., Montero, M. & Alvarez, J. 1999. Ca^{2+}-induced Ca^{2+} release in chromaffin cells seen from inside the ER with targeted aequorin. *J Cell Biol* **144**, 241–254.

Alvarez, Y.D., Ibanez, L.I., Uchitel, O.D. & Marengo, F.D. 2008. P/Q Ca^{2+} channels are functionally coupled to exocytosis of the immediately releasable pool in mouse chromaffin cells. *Cell Calcium* **43**, 155–164.

Artalejo, C.R., Henley, J.R., McNiven, M.A. & Palfrey, H.C. 1995. Rapid endocytosis coupled to exocytosis in adrenal chromaffin cells involves Ca^{2+}, GTP, and dynamin but not clathrin. *Proc Natl Acad Sci USA* **92**, 8328–8332.

Artalejo, C.R., Elhamdani, A. & Palfrey, H.C. 1996. Calmodulin is the divalent cation receptor for rapid endocytosis, but not exocytosis, in adrenal chromaffin cells. *Neuron* **16**, 195–205.

Artalejo, C.R., Elhamdani, A. & Palfrey, H.C. 2002. Sustained stimulation shifts the mechanism of endocytosis from dynamin-1-dependent rapid endocytosis to clathrin- and dynamin-2-mediated slow endocytosis in chromaffin cells. *Proc Natl Acad Sci USA* **99**, 6358–6363.

Burgoyne, R.D. 1995. Fast exocytosis and endocytosis triggered by depolarisation in single adrenal chromaffin cells before rapid Ca^{2+} current run-down. *Pflugers Arch* **430**, 213–219.

Clayton, E.L., Evans, G.J. & Cousin, M.A. 2007. Activity-dependent control of bulk endocytosis by protein dephosphorylation in central nerve terminals. *J Physiol* **585**, 687–691.

Clayton, E.L., Evans, G.J. & Cousin, M.A. 2008. Bulk synaptic vesicle endocytosis is rapidly triggered during strong stimulation. *J Neurosci* **28**, 6627–6632.

Elhamdani, A., Azizi, F. & Artalejo, C.R. 2006. Double patch clamp reveals that transient fusion (kiss-and-run) is a major mechanism of secretion in calf adrenal chromaffin cells: high calcium shifts the mechanism from kiss-and-run to complete fusion. *J Neurosci* **26**, 3030–3036.

Engisch, K.L. & Nowycky, M.C. 1998. Compensatory and excess retrieval: two types of endocytosis following single step depolarizations in bovine adrenal chromaffin cells. *J Physiol* **506**(Pt 3), 591–608.

Fabiato, A. 1983. Calcium-induced release of calcium from the cardiac sarcoplasmic reticulum. *Am J Physiol* **245**, C1–C14.

Fulop, T. & Smith, C. 2006. Physiological stimulation regulates the exocytic mode through calcium activation of protein kinase C in mouse chromaffin cells. *Biochem J* **399**, 111–119.

Fulop, T., Radabaugh, S. & Smith, C. 2005. Activity-dependent differential transmitter release in mouse adrenal chromaffin cells. *J Neurosci* **25**, 7324–7332.

von Gersdorff, H. & Matthews, G. 1997. Depletion and replenishment of vesicle pools at a ribbon-type synaptic terminal. *J Neurosci* **17**, 1919–1927.

Holt, M., Cooke, A., Wu, M.M. & Lagnado, L. 2003. Bulk membrane retrieval in the synaptic terminal of retinal bipolar cells. *J Neurosci* **23**, 1329–1339.

Knight, D.E. 2002. Calcium-dependent transferrin receptor recycling in bovine chromaffin cells. *Traffic* **3**, 298–307.

Koval, L.M., Yavorskaya, E.N. & Lukyanetz, E.A. 2001. Electron microscopic evidence for multiple types of secretory vesicles in bovine chromaffin cells. *Gen Comp Endocrinol* **121**, 261–277.

Langer, G.A. & Peskoff, A. 1996. Calcium concentration and movement in the diadic cleft space of the cardiac ventricular cell. *Biophys J* **70**, 1169–1182.

Linstedt, A.D. & Hauri, H.P. 1993. Giantin, a novel conserved Golgi membrane protein containing a cytoplasmic domain of at least 350 kDa. *Mol Biol Cell* **4**, 679–693.

Maxfield, F.R. & McGraw, T.E. 2004. Endocytic recycling. *Nat Rev Mol Cell Biol* **5**, 121–132.

Neher, E. 1992. Correction for liquid junction potentials in patch clamp experiments. *Methods Enzymol* **207**, 123–131.

Neher, E. & Zucker, R.S. 1993. Multiple calcium-dependent processes related to secretion in bovine chromaffin cells. *Neuron* **10**, 21–30.

Nie, Z., Boehm, M., Boja, E.S., Vass, W.C., Bonifacino, J.S., Fales, H.M. & Randazzo, P.A. 2003. Specific regulation of the adaptor protein complex AP-3 by the Arf GAP AGAP1. *Dev Cell* **5**, 513–521.

Nucifora, P.G. & Fox, A.P. 1998. Barium triggers rapid endocytosis in calf adrenal chromaffin cells. *J Physiol* **508**(Pt 2), 483–494.

Nucifora, P.G. & Fox, A.P. 1999. Tyrosine phosphorylation regulates rapid endocytosis in adrenal chromaffin cells. *J Neurosci* **19**, 9739–9746.

Patzak, A. & Winkler, H. 1986. Exocytotic exposure and recycling of membrane antigens of chromaffin granules: ultrastructural evaluation after immunolabeling. *J Cell Biol* **102**, 510–515.

Perez Bay, A.E., Ibanez, L.I. & Marengo, F.D. 2007. Rapid recovery of releasable vesicles and formation of nonreleasable endosomes follow intense exocytosis in chromaffin cells. *Am J Physiol Cell Physiol* **293**, C1509–C1522.

Perret, E., Lakkaraju, A., Deborde, S., Schreiner, R. & Rodriguez-Boulan, E. 2005. Evolving endosomes: how many varieties and why? *Curr Opin Cell Biol* **17**, 423–434.

Phillips, J.H., Burridge, K., Wilson, S.P. & Kirshner, N. 1983. Visualization of the exocytosis/endocytosis secretory cycle in cultured adrenal chromaffin cells. *J Cell Biol* **97**, 1906–1917.

Rizzoli, S.O. & Betz, W.J. 2005. Synaptic vesicle pools. *Nat Rev Neurosci* **6**, 57–69.

Rosa, J.M., de Diego, A.M., Gandia, L. & Garcia, A.G. 2007. L-type calcium channels are preferentially coupled to endocytosis in bovine chromaffin cells. *Biochem Biophys Res Commun* **357**, 834–839.

Smith, C.B. & Betz, W.J. 1996. Simultaneous independent measurement of endocytosis and exocytosis. *Nature* **380**, 531–534.

Smith, C. & Neher, E. 1997. Multiple forms of endocytosis in bovine adrenal chromaffin cells. *J Cell Biol* **139**, 885–894.

Wu, W. & Wu, L.G. 2007. Rapid bulk endocytosis and its kinetics of fission pore closure at a central synapse. *Proc Natl Acad Sci USA* **104**, 10234–10239.

ZhuGe, R., DeCrescenzo, V., Sorrentino, V., Lai, F.A., Tuft, R.A., Lifshitz, L.M., Lemos, J.R., Smith, C., Fogarty, K.E. & Walsh, J.V. Jr 2006. Syntillas release Ca^{2+} at a site different from the microdomain where exocytosis occurs in mouse chromaffin cells. *Biophys J* **90**, 2027–2037.

Supporting Information

Additional Supporting Information may be found in the online version of this article:

Figure S1. ERMP was plotted against Exo1 value. Each point represents one cell. The graph includes data from all the experimental series included in Figure 5(c). Note that no evident correlation was found between the two variables ($R = -0.1777$, $n = 189$). The opened circles represent the data obtained in our standard condition (50 mM K^+ plus 2 mM Ca^{2+}).

Figure S2. Time course of the spatially-averaged fluorescence (left) and changes in $[Ca^{2+}]$ expressed as $\triangle F/F$ (right) in single cells stimulated with 50 mM K^+ during 30 s and stained with FM 1-43 or the calcium indicator Fluo4 AM, respectively. (a) Cells were preincubated with 20 μM nitrendipine during 15 min and the drug was mantained throughout the stimulus. (b) Cells were preincubated with 100 mM ryanodine during 15 min and the drug was maintained throughout the

stimulus. (c) Cells were preincubated with 1 μM thapsigargin during 45 min, and the drug was maintained throughout the stimulus. Arrows indicate the last point before the stimulus.

Figure S3. The bar diagram represents the average values of Exo1, Endo, Exo2 and NRF from cells (n = 34) in which Exo1 was induced by application of a 50 mM K^+ during 30 s, but replacing $CaCl_2$ with equimolar $BaCl_2$ (2 mM) in the bath solution. *$P < 0.05$.

Figure S4. Images of chromaffin cells fixed at the end of the protocol described in Materials and Methods, permeabilized and blocked with normal goat serum. Immunostainig were performed with 1 : 500 dilutions of 405 alexa-conjugated anti-rabbit and anti-mouse antibodies. No primary antibodies were applied. As expected, no signal from these antibodies was observed. Columns contain images from the same cell with the signal of FM 1-43 (upper), the antibody (middle) or both (bottom).

Figure S5. The bar diagram represents the average values of Exo1, Endo, Exo2 and NRF for experiments (n = 25) in which Exo1 was induced by application of a 200 μM nicotine during 30 s but in presence of 100 nM bisindolylmaleimide-1 (Bis I).

Please note: Wiley-Blackwell are not responsible for the content or functionality of any supporting materials supplied by the authors. Any queries (other than missing material) should be directed to the corresponding author for the article.